IEEE Access
Multidisciplinary | Rapid Review | Open Access Journal

Received 20 February 2024, accepted 11 March 2024, date of publication 13 March 2024, date of current version 23 April 2024.

Digital Object Identifier 10.1109/ACCESS.2024.3377457

RESEARCH ARTICLE

Optimal Medium-Term Electricity Procurement for Cement Producers

JOSÉ ARELLANO, MIGUEL CARRIÓN, (Member, IEEE), AND ÁLVARO GARCÍA-CEREZO, (Member, IEEE)
Department of Electrical Engineering, Universidad de Castilla–La Mancha, 45071 Toledo, Spain

Corresponding author: Miguel Carrión (miguel.carrion@uclm.es)

This work was supported in part by under Grant PID2021-126566OB-I00, funded by the Spanish Ministry of Science and Innovation MCIN/AEI/10.13039/501100011033, and by ERDF, EU ''A way of making Europe'', under Grant 2022-GRIN-34074 and Grant 2022-GRIN-34260; in part by the Universidad de Castilla-La Mancha, under the UCLM Research Group Program, and in part by the European Commission, under the ERDF.

ABSTRACT In the current economic and energy situation, it is imperative for major electricity consumers to meticulously determine their electricity procurement. This is the case for cement producers. This work intends to determine the most efficient approach to electricity acquisition, considering their involvement in the electricity pool, power-purchase agreements, and the potential installation of a photovoltaic self-production unit and a battery storage system. To achieve this, we model the electricity consumption flexibility of cement producers, accounting for all production processes associated with cement and clinker manufacturing. This results in the formulation of a mid-term decision-making problem under uncertainty, which is addressed through the application of a two-stage risk-averse stochastic programming formulation. In order to reduce the computational size of the resulting optimization problem, the planning horizon is characterized by a set of representative periods obtained through a procedure based on chronological time-period clustering. To analyze the practical viability of the proposed approach, a realistic case study is solved featuring an existing cement producer, real-world energy pool prices, and data pertaining to renewable energy production. The findings derived from this case study highlight the viability of installing a photovoltaic self-production unit as a strategic measure to reduce the expected procurement expenses for the cement producer. Moreover, the photovoltaic self-production unit proves instrumental in mitigating the vulnerability to elevated procurement costs. It has been also observed that an imprecise modeling of the technical characteristics within the cement manufacturing processes can lead to a substantial underestimation of procurement costs.

INDEX TERMS Large electricity consumer, power purchase agreements, cement plant, self-generation facility, stochastic programming.

NOTATION

The notation used throughout this paper is included below for quick reference.

Sets and Indices

$A^M_{pm\omega}$	Set of time periods in which the maintenance period m associated with process p can start in scenario ω
C	Set of contracts, indexed by c
K	Set of period groups used to compute the costs associated with the power capacity and energy purchases in the pool, indexed by k
M_p	Set of maintenance periods of process p, indexed by m
P	Set of processes, indexed by p
P^A_p	Set of ancestor processes whose outputs are directly connected to process p
T	Set of time periods, indexed by t
$T_{k\omega}$	Set of time periods belonging to period group k in scenario ω
T^F	Single-element set composed by the last time period of the planning horizon
Ω	Set of scenarios, indexed by ω

Parameters

$A^{PV}_{t\omega}$	Availability of PV self-generation unit in period t at scenario ω (pu)

The associate editor coordinating the review of this manuscript and approving it for publication was Ahmed A. Zaki Diab.

C_p^E	Average electricity consumption associated with process p (MWh/ton)
C_k^G	Cost of the power contracted with the grid for period group k (€/MW)
$C^{I,PV}$	Annualized investment cost of PV self-generation unit (€/MW)
$C^{I,SE}$	Annualized investment cost of the energy component of the battery system (€/MWh)
$C^{I,SP}$	Annualized investment cost of the power component of the battery system (€/MW)
$C^{U,Or}$	Penalization cost of the non-provision of products requested by clients (€/ton)
D^B	Base demand of auxiliary processes (MW)
D_p^{max}	Maximum power consumption associated with process p (MW)
D_p^{min}	Minimum power consumption associated with process p (MW)
$D_{pt\omega}^{Or}$	Product sale orders requested by clients manufactured by process p at period t and scenario ω (ton/h)
DT_p	Minimum down time associated with process p (h)
$DT'_{pt\omega}$	Auxiliary parameter used to compute the minimum down time in period t associated with process p and scenario ω (h)
$M_{p'p}^T$	Per unit value of product obtained from process p' that is transformed to the final product of process p (pu)
N_T	Number of time periods in the planning horizon
$P_{max,c}^C$	Maximum power capacity that can be signed from contract c (MW)
$P_{max}^{I,PV}$	Maximum power capacity that can be installed of the self-generation PV facility (MW)
S_p^{max}	Maximum quantity of product that can be stored in the storage associated with process p (ton)
S_p^{min}	Minimum quantity of product that can be stored in the storage associated with process p (ton)
T_{pm}^M	Duration of the maintenance period m associated with process p (h)
$T_{pmt\omega}^{M'}$	Auxiliary parameter used to compute the duration of the maintenance period m of process p if starts at period t in scenario ω (h)
UT_p	Minimum up time associated with process p (h)
$UT'_{pt\omega}$	Auxiliary parameter used to compute the minimum up time in period t associated with process p and scenario ω (h)
α	Confidence level (pu)
β	Weighting factor of the risk aversion experienced by the cement producer (pu)
$\gamma^{S,E}$	Minimum energy that can be stored in the battery (pu)
$\gamma^{S,O}$	Initial and final amount of energy stored in the battery (pu)
$\Delta_{t\omega}$	Duration of period t in scenario ω (h)
η^S	Charging and discharging efficiencies of the battery (pu)
λ_c^C	Purchasing energy price of contract c (€/MWh)
$\lambda_{t\omega}^P$	Final purchasing price at the pool considering grid charges and tolls in period t at scenario ω (€/MWh)
$\lambda_{t\omega}^S$	Selling price at the pool in period t at scenario ω (€/MWh)
π_ω	Probability of scenario ω (pu)

Variables

$d_{pt\omega}$	Average power demand associated with process p and period t in scenario ω (MW)
$d_{pt\omega}^{U,Or}$	Unserved quantity of product p in period t and scenario ω (ton)
$e^{I,SE}$	Energy capacity installed from the battery (MWh)
$e_{t\omega}^S$	Energy stored in the battery in period t and scenario ω (MWh)
$m_{pt\omega}^I$	Quantity of input product used from process p in period t and scenario ω (ton)
$m_{pt\omega}^O$	Quantity of output product produced by process p in period t and scenario ω (ton)
$m_{pt\omega}^S$	Quantity of product obtained from process p that is sold to clients in period t and scenario ω (ton)
p_c^C	Contracted power from contract c (MW)
p_k^G	Contracted power from the grid for period group k (MW)
$p^{I,PV}$	Installed power capacity of the solar PV facility (MW)
$p^{I,SP}$	Power capacity installed from the battery (MW)
$p_{t\omega}^P$	Average power purchased from the pool in period t and scenario ω (MW)
$p_{t\omega}^{PV}$	Average power produced by the solar PV facility in period t and scenario ω (MW)
$p_{t\omega}^S$	Average power sold to the pool in period t and scenario ω (MW)
$p_{t\omega}^{S,C}$	Average power charged to the battery in period t and scenario ω (MW)
$p_{t\omega}^{S,D}$	Average power discharged from the battery in period t and scenario ω (MW)
$s_{pt\omega}$	Quantity of product stored in the storage associated with process p in period t and scenario ω (ton)
$v_{pt\omega}^D$	Binary variable that is equal to 1 if process p is consuming electricity in period t and scenario ω
$v_{pmt\omega}^M$	Binary variable that is equal to 1 if the maintenance m of process p starts at period t and scenario ω
ζ_ω	Auxiliary variable used to compute the difference between the procurement cost of scenario ω and the Value-at-Risk for a confidence level α (€)
ξ	Auxiliary variable whose optimal value is the Value-at-Risk for a confidence level α (€)

I. INTRODUCTION

Minimizing the electricity procurement cost for large consumers holds significant importance as it may directly impact their financial viability. By reducing energy expenses, large consumers can allocate more resources to vital aspects of their operations, including i) innovation, ii) employee well-being, iii) growth initiatives, and iv) improving their overall competitiveness. Additionally, cost reduction efforts may be synchronized with sustainability goals by lowering carbon emissions, which aligns with global environmental objectives and enhances the organization's reputation.

A paradigmatic example of a large consumer is the cement industry. Cement plants are significant electricity consumers due to the energy-intensive processes involved in cement production, which includes high-temperature kilns and grinding equipment. The raw materials and clinker used in cement production need to be crushed, ground, and heated, demanding substantial electrical power, as explained in [1].

A. LITERATURE REVIEW

In contrast to the extensive research on modeling the participation of generating units in electricity markets, there has been a much more limited exploration of electricity procurement for large consumers in the technical literature. Nevertheless, over the past few decades, numerous methodologies have been proposed for determining energy procurement strategies for large consumers. Pioneering studies addressing the electricity procurement of large consumers within liberalized electricity markets were conducted by [2], [3], [4], [5].

Nonetheless, identifying the most advantageous electricity procurement strategies for large consumers remains an ongoing area of investigation. Reference [6] introduced a multi-stage stochastic programming formulation for determining the procurement strategies of large consumers participating in the electricity pool while also being able to enter bilateral contracts with electricity suppliers. In contrast, the authors of [7] proposed a two-stage stochastic formulation that considered large consumers with storage facilities capable of investing in onsite solar PV units. Reference [8] explored the economic feasibility of installing PV self-generation units for large consumers. The authors of [9] simultaneously considered the potential use of PV, wind turbines, micro-turbines, and energy storage by large consumers while modeling the uncertainties associated with electricity prices, loads, and renewable production. The recent work [10] examined the electricity procurement of consumers using hybrid systems composed of photovoltaic, wind power, and fuel cells. Reference [11] proposed a stochastic programming model to decide the power-purchase agreements by large consumers in a medium-term planning horizon.

Most of the works described above consider that the demand is input data that cannot be modified with the objective of reducing electricity procurement costs. However, if the individual processes of the industrial consumer are properly modeled, it is possible to formulate accurately the ability of large consumers to change electricity consumption patterns aiming at reducing electricity procurement costs. In this sense, reference [12] delivered a thorough examination of the latest developments in industrial and commercial demand response. Reference [13] solved a long-term integrated production planning and electricity procurement problem while considering uncertainty in product demand. The authors of [14] concentrated on a steel plant and streamlined its scheduling with the goal of maximizing profits in both the energy and spinning reserve markets. The authors of [15] illustrated how digital twins hold promise in enabling the provision of flexibility services from industrial energy systems. Reference [16] proposed a data-driven procedure to support energy-intensive industrial plants to offer energy flexibility in the joint energy and reserve market.

The electricity procurement of cement plants has been also studied by many authors in the past, such as [17], and continues as an active research topic, for instance, the work presented in [18]. Reference [19] proposed a procedure for delivering essential ancillary services, such as regulation and load following for cement power plants, through the synergy of industrial loads capable of adjusting their power consumption in significant discrete increments and an onsite energy storage device that offers finer-grained power adjustments. The work developed in [20] proposed a bilevel formulation to obtain the equilibrium reached by a number of strategic cement producers through a technological representation of the market.

B. OBJECTIVE AND CONTRIBUTIONS

The aim of this paper is to develop a practical, rigorous, and readily applicable tool for cement plant managers seeking to assess their medium-term electricity procurement while accounting for various sources of uncertainty. The considered electricity procurement options comprise the participation in the energy pool, the installation of a photovoltaic self-generation system, the use of batteries, and the exploration of power-purchase agreements. To ensure well-informed decisions, a mathematical modeling is developed to capture the operational characteristics and electricity consumption patterns of all stages in the cement production process.

To the best of our knowledge, this work provides the first mathematical formulation of the medium-term electricity procurement for cement producers considering the scheduling of the production processes. Consequently, this work offers four significant contributions:

1) Formulating the medium-term electricity procurement strategy for a cement plant by providing a precise mathematical description of the operational characteristics of each stage in the cement production process.
2) Modeling the plant's electricity consumption resulting from sales orders. This electricity consumption is flexible, and may vary based on the available electricity procurement options for the cement plant operator.
3) Mathematically defining the decision-making problem as a mixed-integer two-stage risk-averse stochastic programming problem. This involves the incorporation

of binary variables associated with the commitment of individual processes and accounting for the operator's degree of risk aversion. Additionally, this formulation determines the optimal scheduling of maintenance periods for critical processes.

4) Conducting a practical case study using a real-world cement plant as a basis, while considering various sets of electricity procurement options. The process of constructing the input data for this case is meticulously described to simplify the application of the proposed tool for cement plant managers.

II. ELECTRICITY CONSUMPTION OF CEMENT FACTORIES

In any industrial business, particularly in the cement industry, understanding the required power in a plant is crucial for estimating electricity costs and formulating budgets for the upcoming years. For this purpose, it is standard practice to install electricity counters in every section, subsection, or primary driver within these types of plants. Assuming the availability of data such as instant power demand (MW), consumption during any given period (MWh), and main production (ton) for each main and intermediate product, easily accessible through an ERP (Enterprise Resource Planning) or SCADA (Supervisory Control and Data Acquisition) software.

Below, we describe the production process for a cement plant.

A. DESCRIPTION OF THE CEMENT PRODUCTION PROCESS

The process of cement production in a typical cement factory can be briefly described as follows:

- *Quarry*: Limestone and clay are extracted from the quarry using small and controlled detonations. Limestone (70%) and clay (30%) are the primary raw materials used to produce cement.
- *Crushing and prehomogenization*: The limestone is crushed in successive phases until it reaches fragments of about 50 mm. Starting from the variable qualities of the stone, a uniform mineral composition is obtained, which is typically referred as the raw mix.
- *Raw*: Raw meal with ideal granulometry is obtained by using vertical roller mills or ball mills.
- *Kiln*: Raw meal passes through the pre-calcination cyclone exchanger, where the residual heat of the furnace gases is used. Raw meal is the subject of a series of physical and chemical transformations that take place in large rotary kilns: drying (up to 150 °C); dehydration of the clay (up to 500 °C); decarbonation (between 550 °C and 1100 °C); and clinkerization (between 1300 °C and 1500 °C). The clinker passes from approximately 1450 °C to approximately 140 °C through refrigeration grids or satellite tubes attached to the kiln, from which the released gases are sent to the drying process.
- *Clinker grinding and cement manufacturing*: Once the additions, gypsum and other additives have been dosed, the materials are milled and homogenised until the final product is obtained: Portland cement.
- *Expeditions*: The final process consists of packaging or bulk shipment.

B. ELECTRICITY CONSUMPTION OF EACH STAGE

According to the stages of cement production described above, the electricity consumption of a cement factory includes the addition of the following elements:

- *Base consumption (BC)*: This is associated with the minimum power needed for the plant to run. They are all the auxiliary consumptions: compressed air network, refrigeration systems, control rooms, and lighting, among others.
- *Quarry and raw materials section (QRM)*: This section comprises all processes, starting the quarries (if any) or from the discharge of incoming raw materials, involving the crushing and transportation to the pre-homogenization stock. Subsequently, the power consumption in this section is substantial, primarily propelled by energy-intensive processes like crushing, grinding, and transportation.
- *Raw mills (RM)*: They comprise the extraction and transport from the raw materials section, and the grinding and transport to the raw meal stock. The electricity consumption in the raw mills is also notably high due to the energy-intensive grinding process and the operation of conveyors, fans, and control systems.
- *Kiln (K)*: The kiln is the core of a cement plant, where raw materials undergo high-temperature processing to form clinker, a crucial component in cement production. Its importance lies in being the central unit responsible for transforming raw materials into the final product, making it a key determinant of the plant's efficiency and product quality. Moreover, it represents the phase with the highest energy consumption per produced ton. This process encompasses the i) extraction and transport from the raw meal stock to the kiln, ii) clinkerization and cooling processes, and iii) transport to the clinker stock.
- *Cement mills (CM)*: The cement mill in a cement plant consumes a considerable amount of electricity during the grinding of clinker and the production of cement. It involves the operation of grinding equipment, conveyors, and fans. It also includes the comsumption associated with the extraction and transport from the clinker stock and the milling and transport to the cement silos.
- *Expedition (E)*: The expedition section involves the final stage of product packaging and transportation. Its electricity consumption primarily stems from the operation of packaging machinery, conveyors, and other auxiliary equipment essential for the efficient packing and dispatch of the finished cement products.

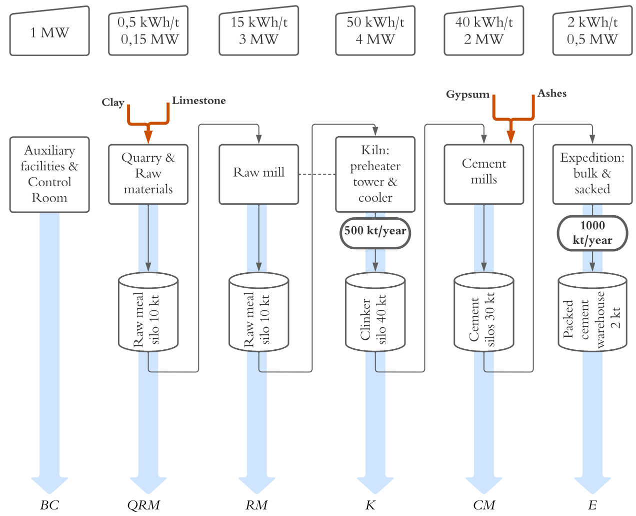

FIGURE 1. **Cement production process.**

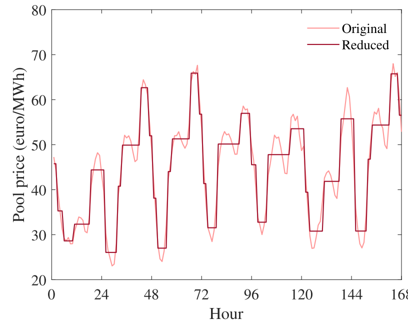

FIGURE 2. **Illustrative example - Original and reduced sets of pool prices.**

Fig. 1 shows the entire cement production process. The electricity consumption of each process, as well as the storage size, is included for a typical plant. Note that the kiln is the most energy-intensive process, exhibiting the highest peak demand and the greatest energy consumption per produced ton.

Given the power consumption profiles outlined above, the challenge for cement plant managers lies in accurately deciding the active consumptions for each hour. This task is contingent on factors such as the performance (ton/h) of each section, storage levels, client orders, and various considerations influencing the decision to operate specific sections. These considerations encompass electricity market prices, scheduled maintenance shutdowns, production and maintenance shift schedules, self-generation unit production, and other relevant factors. The main idea of the approach presented in this paper is to decide on the electricity procurement of the cement plant while simultaneously optimizing the scheduling of the production processes. Consequently, the operation of the cement plant can be adapted to the previously determined electricity procurement strategy to minimize total costs.

III. DECISION-MAKING FRAMEWORK UNDER UNCERTAINTY

The proposed approach considers a medium-term planning horizon. This planning horizon is represented using a target year divided into a set of periods $t \in T$. The characterization of the planning horizon within a single year serves as a compromise between accurately modeling the operational dynamics of the cement plant and ensuring computational tractability. Indeed, the adoption of a singular target year is a common practice in addressing medium-term decision-making problems, as observed in related works such as [11].

The duration of each time period may vary, not necessarily restricted to one hour, since a clustering procedure explained in Section V-H have been applied to different datasets, such as pool price, to reduce the computational size of the optimization problem. The output data of the clustering technique are reduced series, in which each period comprises one or more adjacent periods from the original series. Hence, the duration of each period t must appear in the formulation of the optimization model in order to attain informed results. Fig. 2 illustrates the performance of the clustering technique. The original data involve 168 hourly values of pool prices, while the reduced data comprise 33 periods with different durations. Note that, although errors can be found in the characterization of the pool prices using the 33 periods, only a 20% of the original data are considered, which translates into significantly less variables and constraints in the optimization problem.

At the beginning of the planning horizon, the cement plant operator must decide on i) the installation of a self-generation PV power unit, ii) signing Power Purchase Agreements (PPAs), and iii) the power capacity to contract with the power utility. A PPA is an off-market agreement between an electricity supplier and a consumer for the physical supply of electricity from renewable sources and mid/long term duration. Any demand not met through the self-generation PV unit and PPAs is fulfilled by purchasing energy from the pool.

All these decisions are made in the presence of multiple uncertainties, primarily related to pool prices and the availability of the self-generation facility. The values of these uncertain parameters for each day and time period can be defined as stochastic processes, as described by [21], and can be represented using a set of scenarios denoted by ω in Ω. For the sake of generality, we consider that the duration of each time period t may vary in each scenario ω. This duration is denoted by $\Delta_{t\omega}$ and is measured in hours. It is important to note that all decisions made at the beginning of the planning horizon remain unaltered across all possible outcomes of these uncertain parameters. With this consideration, a two-stage stochastic programming problem can be formulated to determine the investment and contracting decisions of cement producers while accounting for uncertainty. Fig. 3 visually illustrates this two-stage decision-making process considering N_Ω scenarios.

In this paper, the Conditional Value-at-Risk (CVaR), as introduced by [22], is used to capture the risk aversion experienced by the cement plant. Specifically, CVaR is

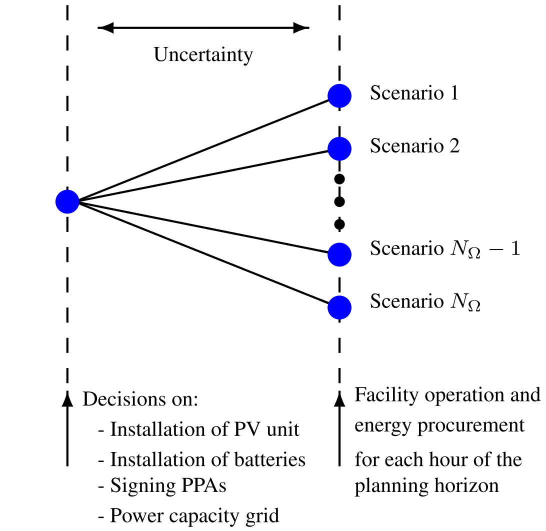

FIGURE 3. Decision-making tree.

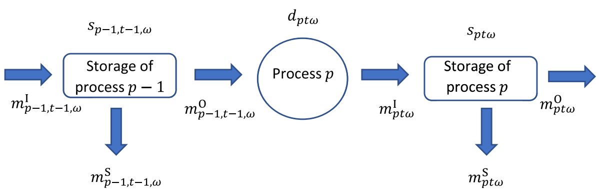

FIGURE 4. Process schema.

here used to measure the expected procurement cost that the cement plant might encounter in the most unfavorable scenarios.

IV. MATHEMATICAL FORMULATION

We define $P \in \{QRM, \ldots, E\}$ as the set of processes p described in Section II-B. Let $m^I_{pt\omega}$ be the variable representing the tons of useful products obtained after process p in period t and scenario ω that are stored for later use. The amount of product stored after process p in period t and scenario ω is denoted by $s_{pt\omega}$, which must be smaller than the storage capacity S^{max}_p and greater than the lower limit S^{min}_p. The quantity of products leaving the storage to feed the next processes is denoted by the variable $m^O_{pt\omega}$, whereas $m^S_{pt\omega}$ is the quantity of product sold to clients in period t and scenario ω. The power consumed by process p in period t and scenario ω is represented by $d_{pt\omega}$. Given the specific processes associated with cement production and the automation of transportation between processes, the material processing time is typically less than one hour. Fig. 4 illustrates the schema of the generic process p.

The set of constraints of the medium-term electricity procurement problem faced by a cement producer are described below.

A. MASS BALANCE OF PRODUCT STORAGES

The mass balance of the storage placed after each process is formulated as follows:

$$s_{pt\omega} = s_{pt-1,\omega} + m^I_{pt\omega} - m^O_{pt\omega} - m^S_{pt\omega}, \quad \forall p, \forall t, \forall \omega \quad (1)$$

$$S^{min}_p \le s_{pt\omega} \le S^{max}_p, \quad \forall p, \forall t, \forall \omega. \quad (2)$$

The amount of product generated after process p depends on the inputs of the products generated in the previous processes that are directly connected to p. This is formulated as:

$$m^I_{pt\omega} = \sum_{p' \in P^A_p} M^T_{p'p} m^O_{p't-1,\omega}, \quad \forall p, \forall t, \forall \omega, \quad (3)$$

where P^A_p is the set of ancestor processes whose outputs are directly connected to process p; parameter $M^T_{p'p}$ indicates the per unit value of the product obtained from process p', which serves as the input product for process p. As mentioned earlier, based on the specific processes involved in the production of cement, all processes require less than one hour to be completed.

The fulfillment of product sale orders, denoted as $D^{Or}_{pt\omega}$ (ton/h), requested by clients, is formulated as:

$$m^S_{pt\omega} = \Delta_{t\omega} D^{Or}_{pt\omega} - d^{U,Or}_{pt\omega} \quad \forall p, \forall t, \forall \omega \quad (4)$$

$$0 \le d^{U,Or}_{pt\omega} \le \Delta_{t\omega} D^{Or}_{pt\omega} \quad \forall p, \forall t, \forall \omega, \quad (5)$$

where $d^{U,Or}_{pt\omega}$ is the unserved demand for the product resulting from process p in period t and scenario ω. Only processes *Kiln* and *Expedition*, whose outputs are clinker and packed cement, respectively, are destined to be sold directly to clients. The amount of clinker that is not sold to clients is used in other processes to produce cement.

B. POWER CONSUMPTION

The average power consumption of process p in period t and scenario ω is denoted as $d_{pt\omega}$ (MW). Each process p is associated with known electricity consumption in MWh per ton, which is denoted as C^E_p. The maximum and minimum electricity consumption per process are determined by the machinery installed in the factory, and they are denoted as D^{max}_p and D^{min}_p (MW), respectively. The mathematical formulation of the energy consumption of process p in period t is:

$$\Delta_{t\omega} d_{pt\omega} \ge C^E_p m^I_{pt\omega}, \quad \forall p, \forall t, \forall \omega \quad (6)$$

$$D^{min}_p v^D_{pt\omega} \le d_{pt\omega} \le D^{max}_p v^D_{pt\omega}, \quad \forall p, \forall t, \forall \omega, \quad (7)$$

where binary variable $v^D_{pt\omega}$ is equal to 1 if the electric equipment associated with process p is in operation in scenario ω, being equal to 0 otherwise. Observe that some equipment may consume electricity even if they are not processing any material. For this reason, constraint (6) is an inequality instead of an equation.

C. MINIMUM UP AND DOWN TIMES OF PROCESSES

Modeling the technical performance of electrical equipment may require the use of a more detailed formulation that considers the establishment of minimum up and down times. Minimum up and down times refer to the specified durations during which an equipment must remain in operation (up time) or be shut down (down time). These predefined time intervals are crucial for ensuring the proper functioning, maintenance, or operational requirements of the equipment. Constraints (8) and (9) formulate the minimum up time, UT_p, and down time, DT_p, considering periods of different duration as follows:

$$\sum_{t'=t}^{UT'_{pt\omega}} \left(v^D_{pt'\omega} - \left(v^D_{pt\omega} - v^D_{pt-1,\omega}\right)\right) \geq 0, \quad \forall p, \forall t, \forall \omega \tag{8}$$

$$\sum_{t'=t}^{DT'_{pt\omega}} \left(1 - v^D_{pt'\omega} - \left(v^D_{pt-1,\omega} - v^D_{pt\omega}\right)\right) \geq 0, \quad \forall p, \forall t, \forall \omega, \tag{9}$$

where $UT'_{pt\omega}$ is the cardinality of the period up to which process p must remain operational upon initiation at period t ($UT'_{pt\omega} = \min((t^*, N_T) \mid t^* = \min\{t^* \mid \sum_{t'=t}^{t^*} \Delta_{t'\omega} \geq UT_p\})$). Conversely, $DT'_{pt\omega}$ denotes the cardinality of the last period for which process p must be inoperative when it is scheduled to shut down at period t, ($DT'_{pt\omega} = \min((t^*, N_T) \mid t^* = \min\{t^* \mid \sum_{t'=t}^{t^*} \Delta_{t'\omega} \geq DT_p\})$). Please note that parameters $UT'_{pt\omega}$ and $DT'_{pt\omega}$ vary with the scenario index ω since the temporal characterization of the year may differ across each scenario under consideration.

D. MAINTENANCE PERIODS

Some processes need to schedule long maintenance periods in which they are not available. The duration of maintenance period m associated with process p is represented by T^M_{pm}. Considering that the duration of time periods can be different in each scenario, the number of time periods that must last the maintenance period m of process p if starts at period t of scenario ω is denoted by $T^{M'}_{pmt\omega}$ (h), the set of periods in which maintenance can be started is $A^M_{pm\omega}$, and the start of the maintenance period m of process p in scenario ω is a decision variable that is mathematically formulated by the binary variable $v^M_{pmt\omega}$. The formulation of the maintenance period is as follows:

$$\sum_{t'=t}^{T^{M'}_{pmt\omega}} \left(v^D_{pt'\omega} - (1 - v^M_{pmt\omega})\right) \leq 0, \quad \forall p, \forall m \in M_p, \forall t \in A^M_{pm\omega}, \forall \omega \tag{10}$$

$$\sum_{t \in A^M_{pm\omega}} v^M_{pmt\omega} = 1, \quad \forall p, \forall m \in M_p, \forall \omega \tag{11}$$

$$v^M_{pmt\omega} = 0, \quad \forall p, \forall m \in M_p, \forall t \notin A^M_{pm\omega}, \forall \omega, \tag{12}$$

where $T^{M'}_{pmt\omega} = \min\{t^* \mid \sum_{t'=t}^{t^*} \Delta_{t'\omega} \geq T^M_{pm}\}$.

E. PHOTOVOLTAIC SELF-GENERATION UNIT

The electricity demand of the plant can be satisfied by installing a PV self-generation unit. The capacity to install $p^{I,PV}$ must be smaller than a maximum value depending on the available space $P^{I,PV}_{max}$. The power production depends on the installed capacity and availability of solar radiation, $A^{PV}_{t\omega}$. This availability is an uncertain parameter that is characterized by a set of scenarios $\omega \in \Omega$.

$$0 \leq p^{PV}_{t\omega} \leq A^{PV}_{t\omega} p^{I,PV}, \quad \forall t, \forall \omega \tag{13}$$

$$0 \leq p^{I,PV} \leq P^{I,PV}_{max}. \tag{14}$$

F. BATTERY OPERATION

Integrating batteries with intermittent self-generation facilities like solar PV plants enables large consumers to optimize energy usage and reduce costs. Additionally, the reduction in the cost of batteries makes them increasingly attractive for industrial and residential applications.

Batteries are mainly characterized by energy and power capacities. The energy capacity refers to the maximum amount of energy that can be stored in the battery. The power capacity is the maximum power that can be either charged to or discharged from the battery. The installed energy and power capacities are denoted by variables $e^{I,SE}$ and $p^{I,SP}$, respectively. The maximum power to charge ($p^{S,C}_{t\omega}$) and discharge ($p^{S,D}_{t\omega}$) the battery in each period t and scenario ω is formulated by constraints (15) and (16), respectively. The limits of stored energy ($e^S_{t\omega}$) are enforced by constraints (17). The energy balance of the battery is established using constraints (18). Parameter η^S refers to the efficiency of charging and discharging the battery. Finally, the minimum level of energy in the battery at the end of the planning horizon is defined by constraint (19).

$$0 \leq p^{S,C}_{t\omega} \leq p^{I,SP}, \quad \forall t, \forall \omega \tag{15}$$

$$0 \leq p^{S,D}_{t\omega} \leq p^{I,SP}, \quad \forall t, \forall \omega \tag{16}$$

$$\gamma^{S,E} e^{I,SE} \leq e^S_{t\omega} \leq e^{I,SE}, \quad \forall t, \forall \omega \tag{17}$$

$$e^S_{t\omega} = e^S_{t-1,\omega} + \eta^S \Delta_{t\omega} p^{S,C}_{t\omega} - \Delta_{t\omega} p^{S,D}_{t\omega} / \eta^S, \quad \forall t, \forall \omega \tag{18}$$

$$\gamma^{S,O} e^{I,SE} \leq e^S_{t\omega}, \quad \forall t \in T^F, \forall \omega. \tag{19}$$

G. POWER-PURCHASE AGREEMENTS

A cement plant can procure part of its demand by signing power-purchase agreements, which are bilateral contracts with electricity suppliers. The power contracted through contract c is denoted by p^C_c (MW). The purchasing price of electricity associated with PPA c is λ^C_c (€/MWh). For simplicity, this formulation considers PPAs spanning the entire target year. More complex PPA configurations are detailed in [11]. The limits of the power purchased through PPA contracts are formulated as follows:

$$0 \leq p^C_c \leq P^C_{max,c}, \quad \forall c. \tag{20}$$

H. POWER DEMAND PROCUREMENT

The power demand procurement for the plant is formulated in this subsection. Variables $p^P_{t\omega}$ and $p^S_{t\omega}$ denote the power purchased from and sold to the pool, respectively. Equation (21) formulates the power balance for each period t and scenario ω, where D^B represents the base power consumption of auxiliary elements. Constraints (22) and (23) ensure the positive nature of power purchased from and sold to the pool. Variable p_k^G models the power capacity contracted with the grid operator, with tariffs typically distinguishing between different types of periods, $k \in K$, and associated different prices. Constraints (24) and (25) establish that the power capacity contracted with the grid must exceed the power injected and extracted from the grid in each time period and scenario, respectively.

$$p_{t\omega}^P + \sum_{c \in C} p_c^C + p_{t\omega}^{PV} + p_{t\omega}^{S,D} = \sum_{p \in P} d_{pt\omega} + D^B + p_{t\omega}^{S,C} + p_{t\omega}^S, \quad \forall t, \forall \omega \tag{21}$$

$$p_{t\omega}^P \geq 0, \quad \forall t, \forall \omega \tag{22}$$

$$p_{t\omega}^S \geq 0, \quad \forall t, \forall \omega \tag{23}$$

$$p_k^G \geq p_{t\omega}^P + \sum_{c \in C} p_c^C, \quad \forall k, \forall t \in T_{k\omega}, \forall \omega, \tag{24}$$

$$p_k^G \geq p_{t\omega}^S, \quad \forall k, \forall t \in T_{k\omega}, \forall \omega. \tag{25}$$

I. CONDITIONAL VALUE-AT-RISK

The risk assessment metric used in this formulation is the Conditional Value-at-Risk at a specified confidence level α (α-CVaR) [22]. When dealing with a discrete cost distribution, α-CVaR serves as an approximation of the expected cost associated with the most costly scenarios. The α-CVaR is determined through variables ξ and ζ_ω as $\xi + \frac{1}{1-\alpha} \sum_{\omega \in \Omega} \pi_\omega \zeta_\omega$.

The optimal value of ξ represents the smallest value such that the probability that the cost exceeds or equals it is less than or equal to $1 - \alpha$, i.e., the Value-at-Risk (VaR). Additionally, ζ_ω is the difference between the procurement cost of scenario ω and the VaR. The values of variables ξ and ζ_ω are determined by the following set of constraints:

$$\sum_{k \in K} C_k^G p_k^G + C^{I,PV} p^{I,PV} + C^{I,SE} e^{I,SE} + C^{I,SP} p^{I,S} + \sum_{t \in T} \Big(\lambda_{t\omega}^P \Delta_{t\omega} p_{t\omega}^P - \lambda_{t\omega}^S \Delta_{t\omega} p_{t\omega}^S + \sum_{c \in C} \lambda_c^C \Delta_{t\omega} p_c^C + \sum_{p \in P} C_{pt\omega}^{U,Or} d_{pt\omega}^{U,Or} \Big) - \xi \leq \zeta_\omega, \quad \forall \omega, \tag{26}$$

$$\zeta_\omega \geq 0, \quad \forall \omega. \tag{27}$$

The summation of terms on the left-hand side of constraint (26), excluding variable ξ, represents the total procurement cost associated with scenario ω. This cost encompasses the i) annual cost of power contracted from the grid, ii) the annualized investment cost of the PV self-generation unit, iii) the annualized investment costs of energy and power components of the battery, iv) the annual cost associated with energy purchased from the pool, v) the negative anual revenue from energy sold to the pool, vi) the cost associated with the annual energy purchased from PPAs, and vii) the annual penalization cost of unserved sale orders requested by clients.

J. OBJECTIVE FUNCTION

The objective of this problem is to minimize the total cost incurred by the cement power plant plus the CVaR.

The objective function (28) is composed of two terms, each of them weighted by the parameters β and $(1 - \beta)$. The parameter β represents a weighting factor that falls within the range of [0,1] and serves the purpose of characterizing the level of risk aversion experienced by the cement producer.

The component multiplied by β signifies the expected procurement cost. Meanwhile, the term multiplied by $(1 - \beta)$ corresponds to the CVaR, which quantifies the risk associated with incurring higher costs and is approximately equivalent to the expected cost within the $(1 - \alpha)$ worst-case scenarios, as outlined in [22].

Consequently, when $\beta = 1$, the CVaR term is disregarded, and the cement producer behaves as a risk-neutral entity, aiming to minimize the expected cost without considering the expenses linked to the worst-case scenarios. Conversely, with $\beta = 0$, the expected cost component is excluded, and the cement producer operates as a risk-averse entity, striving to minimize the costs within the worst-case scenarios as extensively as possible.

The total expected cost comprises the summation of scenario-independent costs along with the expected cost of those dependent on the scenario. Scenario-independent costs include the annual cost of power contracted from the grid, the annualized investment cost of the PV self-generation unit, and the annualized investment costs of energy and power components of the battery. In contrast, the expected cost of scenario-dependent costs incorporates the expected value of the summation of scenario-dependent costs, such as the annual cost associated with energy purchased from the pool, the negative annual revenue from energy sold to the pool, the cost associated with the annual energy purchased from PPAs, and the annual penalization cost of unserved orders requested by clients. The expected cost is calculated as the weighted sum of the cost in each scenario multiplied by its occurrence probability.

$$\text{Minimize}_{\Theta} \; \beta \Bigg(\sum_{k \in K} C_k^G p_k^G + C^{I,PV} p^{I,PV} + C^{I,SE} e^{I,SE} + C^{I,SP} p^{I,S} + \sum_{\omega \in \Omega} \pi_\omega \Big[\sum_{t \in T} \Big(\lambda_{t\omega}^P \Delta_{t\omega} p_{t\omega}^P - \lambda_{t\omega}^S \Delta_{t\omega} p_{t\omega}^S + \sum_{c \in C} \lambda_c^C \Delta_{t\omega} p_c^C + \sum_{p \in P} C_{pt\omega}^{U,Or} d_{pt\omega}^{U,Or} \Big) \Big] \Bigg) + (1 - \beta) \Bigg(\xi + \frac{1}{1 - \alpha} \sum_{\omega \in \Omega} \pi_\omega \zeta_\omega \Bigg) \tag{28}$$

where set $\Theta = \{d_{pt\omega}, d_{pt\omega}^{U,Or}, e^{I,SE}, e_{t\omega}^{S}, m_{pt\omega}^{I}, m_{pt\omega}^{O}, m_{pt\omega}^{S}, p_c^C, p_k^G, p^{I,PV}, p^{I,SP}, p_{t\omega}^{P}, p_{t\omega}^{PV}, p_{t\omega}^{S}, p_{t\omega}^{S,C}, p_{t\omega}^{S,D}, s_{pt\omega}, v_{pt\omega}^{D}, v_{pmt\omega}^{M}, \zeta_\omega, \xi\}$ includes the optimization variables.

K. TIME-PERIOD CLUSTERING, SCENARIO REDUCTION AND SOLUTION PROCEDURE

Problem (1)-(28) constitutes a large-scale mixed-integer linear programming formulation of the two-stage risk-averse stochastic programming model for the medium-term electricity procurement problem faced by a cement producer. This model addresses the uncertainties associated with pool prices and the availability of the PV self-production unit.

The large number of constraints and the combination of continuous and binary variables in problem (1)-(28) may pose challenges for efficient solving. Therefore, a clustering procedure is employed to mitigate this issue by reducing the number of periods used to characterize the target year. Additionally, a scenario reduction technique is applied to decrease the number of scenarios while ensuring sufficient characterization of uncertain parameters. The resulting problem is then solved in three sequential steps, aimed at significantly diminishing solution times.

1) CHRONOLOGICAL TIME-PERIOD CLUSTERING

In order to reduce the computational size of the resulting optimization problem, the initial planning horizon of 8760 hourly periods has been reduced to a number of representative periods through a procedure based on the chronological time-period clustering (CTPC) described in [23]. Unlike most of the clustering techniques, the CTPC provides a set of representative periods that maintain the chronological sequence among them throughout the entire planning horizon. This is key in our work since inter-temporal constraints have been considered, i.e., constraints (1), (3), (8), (9), (10), (11), (18), and (26). The CTPC have been applied for each scenario ω following these steps:

1) The desired number of periods is selected. This number should be selected with the aim of finding a trade-off between the computational burden of the optimization problem and the accuracy of the representation of the input data.
2) Input data, which involves data of pool prices and self-generation PV availability from scenario ω, are normalized by using the min-max normalization [24]. This normalization process is needed when different series are considered as input data.
3) The two adjacent periods with minimum dissimilarities of the input data between them are merged. The duration $\Delta_{t\omega}$ of the resulting period t is equal to the sum of the two merged periods' durations. The reader is kindly referred to [23] for further information about the calculation of the dissimilarities.
4) If the number of periods is equal to the number selected in Step 1), stops. Otherwise, go to Step 3).

The resulting periods should be linked to values of the four time series considered as input data of the optimization problem, i.e., pool prices ($\overline{\lambda}_{t\omega}^{P}$), self-generation PV availability ($A_{t\omega}^{PV}$), and clinker and cement demands ($D_{t\omega}^{Or}$). Note that each resulting period t is associated with a cluster that comprises one or more adjacent periods from the original historical series, i.e., those periods that have been merged leading to period t. Hence, the data of the new periods are computed as the centroids of the historical data within their clusters for each time series, period t and scenario ω. It is worth mentioning that the clustering procedure have been carried out considering that only the pool prices and the solar PV availability are the input data of the CTPC, rather than using the four time series mentioned above. The reason behind this lies in the presence of large clinker and cement storages, which means that individual high or low hourly sales at a particular hour do not significantly impact the scheduling and operation of cement plant processes. However, high or low values of pool prices or solar availability at a particular hour may influence the initiation or shutdown of different processes.

2) SCENARIO REDUCTION

For the sake of tractability, the set of scenarios used to represent pool prices and solar PV availability may be reduced by using a scenario reduction trying to reach a compromise between accuracy and tractability. In this work, we propose to use the algorithm described in [25], which is based on solving the full optimization problem (1)-(28) as many times as scenarios are initially generated considering only one scenario each time. Afterwards, scenarios are selected according to the expected cost associated with each single scenario.

While this technique involves a higher computational load compared to alternative methods, it remains manageable. The computational cost of solving single-scenario instances is relatively low and can be parallelized. The primary advantage of this approach is its consideration of the influence of uncertain parameters (e.g., pool prices and solar PV availability in this problem) on the objective function during the scenario reduction process. Subsequently, scenarios with similar costs are identified for potential merging, proving particularly advantageous in reducing scenarios with different uncertain parameters, where the impact of these parameters on the objective function may not be identical.

3) SOLUTION PROCEDURE

Although the CPTC procedure and scenario-reduction techniques can be employed to mitigate computational complexity, the substantial quantity of binary variables in problem (1)-(28) poses challenges for efficient resolution. Consequently, we introduce a three-step procedure to address and solve the problem:

- *Step 1*: The initial phase involves solving a continuous linear-programming relaxed version of (1)-(28). This step determines first-stage variables, including the installed capacities of the PV self-generation unit, power and energy components of batteries, and contracted power to the grid. In particular, the problem solved in this phase corresponds to (1)-(7), (13)-(28), wherein binary variables v^{D}_{ptw} are relaxed, allowing them to assume continuous values within the interval [0, 1]. This problem is solved very fast (few minutes).

- *Step 2*: Subsequently, the original problem, (1)-(28), is solved with the first-stage variables fixed based on the outcomes of the preceding step. Since first-stage variables are fixed, this problem is solved significantly faster than the original problem (in which first-stage variables must be determined).
- *Step 3*: The solution derived from *Step 2*, which is a feasible solution of problem (1)-(28), is utilized as a warm start for the final resolution of the original problem to speed up the solution process.

L. TOOL USAGE AND LIMITATIONS

The proposed decision-making tool is based on a static decision approach formulated using a two-stage stochastic programming model. This technique has been used in the proposed approach because the most relevant uncertain parameter in this problem, pool prices and solar PV availabilities, can be easily characterized using scenarios and the decision-making process of the consumer can be modeled using a two-stage approach. Investment decisions, and contracting decisions related the PPAs and the grid power capacity may be revised and updated on a desired time basis as the tool is intended to be used dynamically as many times as required by the cement plant manager. To do so, information on new generation and storage technologies, or candidate PPAs can be incorporated into the model, as well as an updated estimation of future pool prices and the cement plant demand. It is also important to note that the formulation proposed for this tool does not assume any specific values for the technical characteristics of the cement plant stages, and is specially designed to be versatile and applicable to any cement producer.

Observe that the proposed tool is subjected to several limitations. The first limitation of this tool is its dependence on a set of realistic electricity prices and solar production values to facilitate informed decision-making. While obtaining solar production data from historical records is relatively straightforward, estimating pool prices may necessitate the development of a dedicated tool or engagement with a company specialized in electricity price estimations. Another limitation pertains to the static nature of the decision-making procedure, where all investment decisions are made within a single period. The advantage of this static approach lies in its simplicity of formulation and significantly reduced computational complexity, easing the problem-solving process. Static models, by design, eliminate the need to estimate uncertainties associated with random variables in future time periods, a challenge often encountered in dynamic models. However, it is crucial to acknowledge the downside of static models, since they lack the flexibility to consider alternative decisions in subsequent time periods. This limitation is accepted as part of the trade-off between simplicity and the consideration of evolving conditions over time. The final limitation of the model lies in the computational size of the resultant optimization model. Given the incorporation of binary variables linked to scenario and time period indices, the number of binary variables escalates linearly with the expansion of scenarios and time periods. Consequently, while there are no significant time restrictions in solving these types of medium-term planning models, when dealing with practical problems involving hundreds of thousands of variables and constraints, the computational time required for solving such models may extend to durations exceeding 24 hours.

V. CASE STUDY

We conducted a practical case study to evaluate the proposed formulation. In this instance, we consider a cement manufacturer situated in central Spain. Specific details about this consumer are withheld for confidentiality purposes. The analysis covers a medium-term planning horizon represented by a single year. Please note that the objective of this case study is to validate the proposed mathematical formulation rather than provide general conclusions applicable to any cement plant. It is important to acknowledge that variations in cement plant configurations or different input data values may yield different qualitative results regarding the selection of electricity procurement options.

A. CLINKER AND CEMENT DEMANDS

The clinker and cement demands are derived from actual data pertaining to the reference cement plant. To determine the final demand, we consider monthly, daily, and hourly data. Initially, we analyze the monthly demand for clinker and cement. Following this, we extrapolate daily and hourly demand per unit and convert the monthly quantity values to obtain corresponding hourly quantities. These values are then rounded to align with the standard practice of utilizing 25-ton trucks for the transportation of clinker and cement from the manufacturing plant to their designated destinations. Fig. 5 illustrates the monthly, daily, and hourly values as described above. It is worth noting that identical daily and hourly per-unit quantities apply to both clinker and cement. For instance, Fig. 6 depicts the hourly demand for cement throughout the year. In this case study, we consider total annual demands of 295 thousand metric tons for cement and 145 thousand metric tons for clinker.

B. CEMENT AND CLINKER PRODUCTION PROCESSES

Table 1 provides details for each process outlined in Section II-B, including energy consumption per ton produced, maximum and minimum power consumption, and storage capacity. It is considered that the minimum amount of product that can be stored at any given time should be at

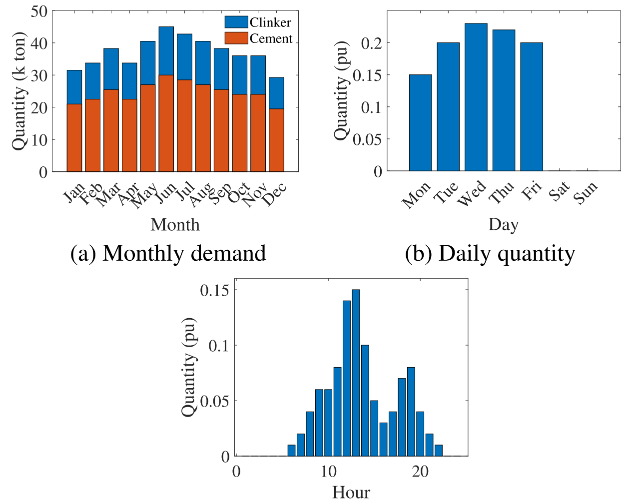

(a) Monthly demand (b) Daily quantity

(c) Hourly quantity

FIGURE 5. Clinker and cement demands.

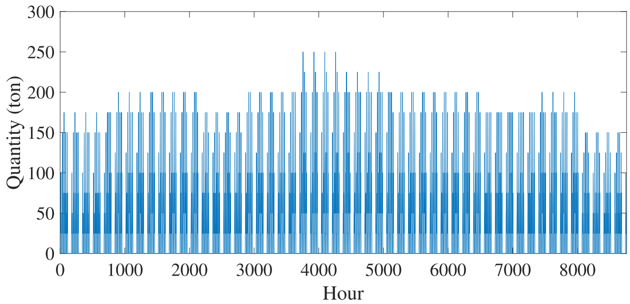

FIGURE 6. Hourly cement demand.

TABLE 1. Processes description.

Process	Energy consump. (kWh/ton)	Max. power consump. (kW)	Min. power consump. (kW)	Storage capacity (ton)
BC	-	1000	-	
QRM	0.5	150	0	12000
RM	15	3000	0	12000
K	50	4000	3600	60000
CM	40	2000	0	60000
E	2	500	0	6000

least 20% of the maximum capacity. Additionally, the initial quantity of product stored at the beginning of the planning horizon is set to 50% of the storage capacity.

Table 2 outlines the elements of the matrix $M^T_{p'p}$, which indicate the per unit value of the product obtained from process p' that transforms into the final product of process p. For example, the input-output material matrix has a value of 0.9, representing the transition between the QRM and RM. This value is influenced by the material drying process in the raw mill, resulting in a 10% weight loss due to reduced humidity. Notably, the main conversion takes place during the transition from RM to K, characterized by decarbonation ($CaCO_3 \rightarrow CaO + CO_2$), resulting in roughly 60 tons of clinker for every 100 tons of feed, as depicted in Table 2.

TABLE 2. Input-output material matrix (pu).

Process	RM	K	CM	E
QRM	0.9	0	0	0
RM	0	0.6	0	0
K	0	0	1	0
CM	0	0	0	1

TABLE 3. Power capacity toll per period group and year.

Period group	1	2	3	4	5	6
$\overline{C}^G_k$ (€/kW)	15.917	13.734	7.909	5.283	2.297	1.436

The kiln undergoes two extense maintenance periods annually. The first spans 14 days, commencing between April 1^{st} and May 31^{st}, while the second extends over 25 days, starting from October 1^{st} to December 10^{th}. Furthermore, to prevent mechanical deterioration of the kiln, and to optimize the costs of heating and cooling it, minimum up and down times are set at 28 and 14 days, respectively.

C. CONTRACTED POWER TO THE GRID OPERATOR

In this case study, the contracted power expenses are determined by Tariff 6.3 TD, a pricing structure specifically designed for industrial consumers within the Spanish power system [26]. This tariff classifies consumption into six distinct periods denoted by $k \in \{1, \cdots, 6\}$.

The cost associated with the contracted power for each group period k, C^G_k, is computed as:

$$C^G_k = 1000 \times \overline{C}^G_k \times (1 + ET) \times (1 + VAT), \quad \forall k, \quad (29)$$

where ET represents the electric tax at a rate of 5.113%, VAT denotes the value-added tax at 21%, and the parameter $\overline{C}^K_k$ corresponds to the cost associated with each period group in Tariff 6.3 TD, as outlined in Table 3. This particular tariff is the standard one used by cement producers in Spain according to their required voltage and peak power consumption.

D. POOL PRICES

Pool prices exhibit stochastic behavior, representing a dynamic process. For instance, Fig. 7 provides the boxplot representation of pool prices for each year between 2008 and 2020, specific to the Spanish power system [27]. Within each box, the central line indicates the median price, while the upper and lower edges of the box signify the 75th and 25th percentiles, respectively. The whiskers extend to display the range within which 99.3% of prices fall if they follow a normal distribution. Any gray points positioned beyond the whiskers are considered outliers. This visual representation reveals that there is a substantial year-to-year uncertain price variability. To capture this uncertainty, we consider three distinct scenarios, each corresponding to historical pool prices extracted from the dataset considered in Fig. 7. The selected scenarios correspond to prices in years 2008, 2012 and 2020. Observe that year 2012 corresponds

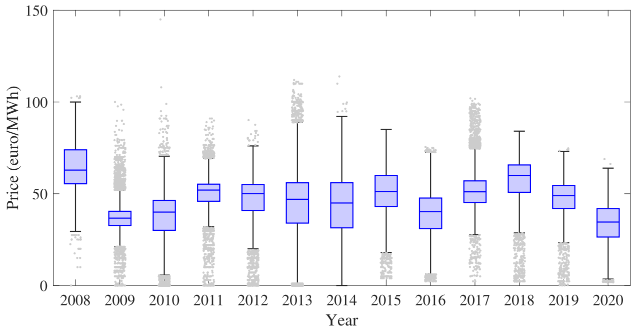

FIGURE 7. Historical pool prices.

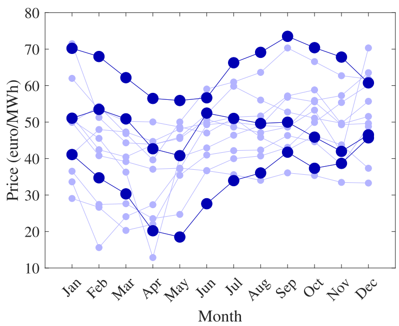

FIGURE 8. Monthly average pool prices for selected scenarios.

TABLE 4. Energy, capacity and losses terms.

Period group	1	2	3	4	5	6
E_k^T (€/kWh)	0.021974	0.017208	0.009868	0.004756	0.001845	0.001250
C_k^T (€/kWh)	0.001031	0.000476	0.000317	0.000238	0.000238	0.000000
L_k^T (%)	4.2	4.3	4.0	4.0	3.0	4.4

to the year with average pool prices, whereas minimum and maximum prices were observed in years 2020 and 2008, respectively. The monthly average value of selected scenarios are represented in dark blue in Fig. 8. Non-selected scenarios, which are associated with the remaining years between 2008 and 2020, are depicted in light blue color. The probability of each scenario is assigned according to the procedure described in [28].

The final purchasing price of electricity by the cement producer in the pool, $\lambda^P_{t\omega}$, depends on pool prices $\overline{\lambda}^P_{t\omega}$ as follows:

$$\lambda^P_{t\omega} = \left(\overline{\lambda}^P_{t\omega} + 1000 \times \left(E^T_k + C^T_k \times (1 + L^T_k/100)\right)\right) \times (1 + ET) \times (1 + VAT), \quad \forall k, \forall t \in T_{k\omega}, \forall \omega, \quad (30)$$

where E^T_k (€/kWh), C^T_k (€/kWh), and L^T_k (%) are energy, capacity and losses terms used to pay for the usage of the networks, which values for Tariff 6.3 TD are included in Table 4.

The selling price of the electricity surplus by the cement producer in the pool, $\lambda^S_{t\omega}$, is calculated as:

$$\lambda^S_{t\omega} = \overline{\lambda}^P_{t\omega} \times (1 - ST), \forall t, \forall \omega, \quad (31)$$

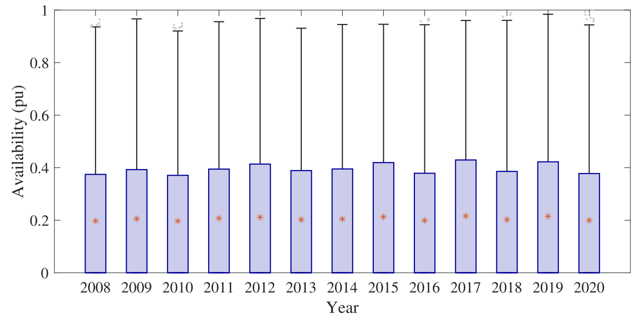

FIGURE 9. Historical solar PV availability.

where ST is the special tax for electricity generation, and it is equal to 7%.

E. POWER PURCHASE AGREEMENTS

In this case we consider three different PPAs that can be signed by the cement plant. All PPAs cover the entire planning horizon and come with a maximum power capacity for contracting set at 2.5 MW. The purchasing prices for these three contracts are equal to 69.92, 76.58 and 83.24 €/MWh, respectively. These values are determined by multiplying the expected pool prices by factors of 1.05, 1.15, and 1.25, respectively.

F. SOLAR PV AVAILABILITY

The solar PV availability at the location of the cement plant is obtained from PVGIS (Photovoltaic Geographical Information System) [29]. This is an online tool developed by the European Institute of Energy and the Environment that provides detailed information about the potential for photovoltaic solar energy in various regions around the world. For this case study, we calculated availability data for a fixed-axis solar panel installation with a 30-degree south-facing slope. The values, derived from historical solar radiation data spanning from 2008 to 2020, are visually represented in Fig. 9 as a boxplot. Taking into account that the median of the annual availability is zero due to a significant number of hours without solar irradiation, the average annual availability for each year is also represented in this figure by a red asterisk. It is notable that the variability in solar production is considerably lower than what we observe in pool prices.

However, even with the overall low annual variability in solar production, when we examine the average monthly availability for each year, a noticeable fluctuation in months with comparatively lower availability is observed, particularly during the winter and spring months. This fact is clearly depicted in Fig. 10a. Consequently, we have concluded that solar PV availability should be characterized as a stochastic process, and we have represented it using three scenarios that correspond to low, high, and average values. Selected scenarios are represented in dark blue color in Fig. 10b. Similarly to the approach used for pool prices, the probability

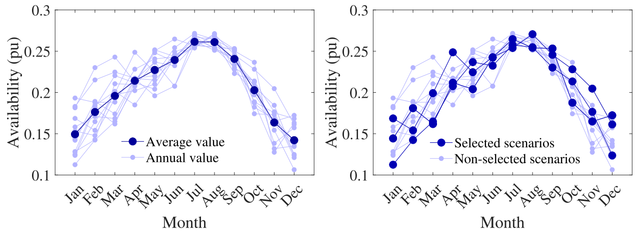

(a) Historical monthly solar PV availability (b) Monthly average solar PV availability for selected scenarios

FIGURE 10. PV availability.

for each scenario is determined following the procedure outlined in [28]. Given that three pool price scenarios are under consideration, this case study encompasses a total of 9 scenarios. Note that in this scenario generation process, it is implicitly assumed that there is no correlation between electricity prices in the day-ahead market in the Spanish power system and the availability of PV production. It is important to emphasize that the solar availability considered here pertains to a specific location and does not reflect the average solar availability across the entire power system.

The maximum capacity that can be installed is 25 MW. Investment costs are annualized using the capital recovery factor formula $\frac{r(1+r)^x}{(1+r)^x-1}$, where r represents the interest rate, and x denotes the lifetime of each considered technology [30]. We consider an interest rate of 3.5% and an expected lifespan of the self-generation PV facility of 20 years.

G. BATTERY

It is assumed that a Li-ion battery can be installed. The capital costs for power and energy components are set at 285 €/kW and 306 €/kWh, respectively [31]. The charge and discharge efficiencies are both 0.9. At any given time, the battery must maintain a minimum energy level equivalent to 15%, and the initial energy state of the battery is 50% of the installed energy capacity. The expected lifespan of the battery is 10 years, and the investment costs are annualized using the method previously specified for the self-generation PV facility.

H. TEMPORAL CHARACTERIZATION

The CTPC, as detailed in Section IV-K, is applied to condense the initial set of 8760 hourly periods representing the year to a more manageable set of 720 periods. This final number has been chosen to strike a balance between computational tractability and the accurate characterization of time-dependent parameters and variables. As an example of the CTPC's performance, Fig. 11 showcases the original and reduced series of pool prices and PV availabilities for scenarios 1, 5, and 9. Note that the 720-period series has been expanded into a 8760-period series by assigning the same values for the series across all hours within periods with a duration greater than one hour. These specific scenarios have been chosen to provide a visual representation of the three distinct pool price scenarios and three PV availability scenarios mentioned in Sections V-D and V-F, respectively.

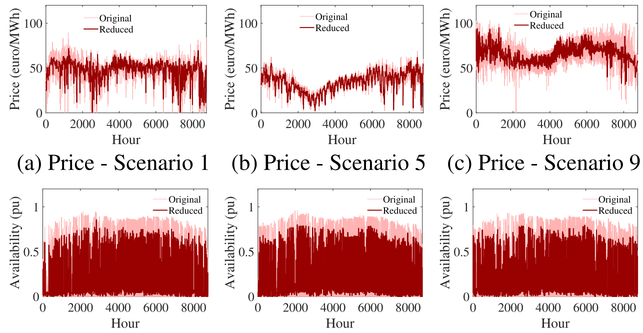

(a) Price - Scenario 1 (b) Price - Scenario 5 (c) Price - Scenario 9

(d) PV - Scenario 1 (e) PV - Scenario 5 (f) PV - Scenario 9

FIGURE 11. Original and reduced sets of pool prices and self-generation PV availabilities in selected scenarios.

This figure shows how the chronological sequence of the original 8760-period series can be adequately reproduced by the 720-period series.

Please note that the parameter $D^{Or}_{pt\omega}$, denoting product sale orders requested by clients, is derived for each scenario through the clustering technique outlined in Section III.

I. SCENARIO REDUCTION

To reduce the computational size of the optimization problem, we employ the scenario reduction technique proposed in [25] and detailed in Section IV-K within this case study. Through this method, the initial number of nine scenarios has been reduced up to five. As outlined in Section IV-K, we solve problem (1)-(28) nine times, each time focusing on a single scenario. The subsequent reduction of scenarios is based on the resultant cost associated with each scenario.

Fig. 12 illustrates the probability mass function of the costs associated with the initial and reduced scenario sets, including the cost of each scenario and its probability. Higher costs align with elevated pool prices and diminished solar PV availability, while lower costs are linked to reduced pool prices and increased solar PV availability.

Fig. 12a reveals visually that cost scenarios are grouped into three sets of three scenarios each. These groups correspond to low, medium, and high pool prices, with each set of scenarios encompassing low, medium, and high solar PV availability. Notably, the costs linked to low and medium solar PV availability for any given pool price are closely aligned. This observation suggests that the influence of pool prices on the costs incurred by the cement producer outweighs that of solar PV availability.

Examining Fig. 12b, the reduced set of scenarios effectively captures the variability in costs observed in the initial scenario set. Furthermore, it is evident that the probabilities associated with removed scenarios are redistributed to scenarios with medium solar PV availability within scenario groups featuring low, medium, and high pool prices.

VI. RESULTS AND DISCUSSION

In this section, we analyze the outcomes obtained through the application of the formulation outlined in Section IV to the previously mentioned case study.

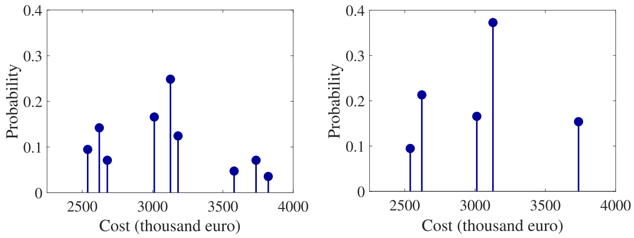

FIGURE 12. Mass probability functions of cost scenarios.

TABLE 5. Expected cost and CVaR (thousand €).

Case	β	Expected cost	CVaR
Rel	1	3045.8	3712.3
	0	3292.9	3452.1
BAU	1	3330.2	4087.3
	0	3879.3	3906.1
OnlyP	0-1	4461.2	5449.8
NoGrid	0-1	9914.4	9914.4

To evaluate the effectiveness of the proposed formulation, we solved four cases:

- *Rel*: All electricity procurement options can be used and binary variables are relaxed (neglecting minimum up and down times and minimum power consumption).
- *BAU*: Business-as-usual scenario where all electricity procurement options can be used.
- *OnlyP*: The entire demand is met through purchases in the pool; neither the PV self-generation unit nor the battery can be installed, and PPAs cannot be contracted.
- *NoGrid*: The cement plant is not connected to the grid, and the entire demand must be supplied by the PV self-generation unit and the battery. In this specific case, the potential capacity to be installed from PV and batteries is considered to be unbounded.

All simulations were executed using CPLEX 12.6.1 on a server equipped with four 3.0 GHz processors and 250 GB of RAM. In the *BAU* case, the number of constraints, continuous variables, and binary variables amounted to 369.5 thousand, 272.2 thousand, and 32.4 thousand, respectively. As an example, the solution times of the three stages described in Section IV-K for solving the *BAU* case were as follows: 35 seconds to address the relaxed instance of the problem, 2.1 hours to resolve the issue with first-stage variables fixed based on the relaxed instance, and 116 hours to tackle the final problem, utilizing the solution obtained from the preceding problem as a warm start.

Table 5 illustrates the expected cost and CVaR for each examined case, considering values of β at both 1 and 0. Instances with $\beta = 1$ signify risk-neutral stances, where decisions rely solely on expected costs. Conversely, $\beta = 0$ indicates risk-averse cases, where decisions are shaped by the worst-case scenarios characterized by the CVaR. Please note that cases *OnlyP* and *NoGrid* yield identical solutions for any value of β. In the instance of *OnlyP*, the absence of alternative sources, apart from the pool, avoids the opportunity to mitigate exposure to cost variabilities. Meanwhile, in the case of *NoGrid*, where participation in the pool is prohibited, costs across all scenarios are uniform. Consequently, the expected value and the CVaR of the costs align.

Observe that the lowest costs are achieved in the *Rel* case, wherein all binary variables used to model the kiln's operation are neglected. Consequently, the expected costs in this case for $\beta = 1$ is reduced by 8.5% compared to that obtained in the *BAU* case. This outcome implies that the simplification of the modeling of the operational processes in the *Rel* case significantly underestimates the costs incurred by the cement plant. In a comparative context, the expected cost in the *BAU* case is 25.3% less than that in the *OnlyP* case. This indicates that relying solely on the pool to fulfill the cement plant's demand is notably more expensive than exploring alternative procurement options, such as the PV unit, as will be discussed later. Lastly, the *NoGrid* case proves to be considerably more expensive than the other cases. This high cost is attributed to the decoupling from the grid, which necessitates substantial investments in the PV unit and batteries needed for the disconnection from the grid.

The results provided by Table 5 also show that the proposed formulation effectively diminishes the expected cost in adverse scenarios modeled by the CVaR when the cement producer exhibits risk aversion ($\beta = 0$). In this context, the risk-averse solution for $\beta = 0$ results in a 7.0% and 4.4% reduction in CVaR for the *Rel* and *BAU* cases, respectively, compared to the cases with $\beta = 1$. However, the reduction in CVaR is nearly negligible for the *OnlyP* and *NoGrid* cases. This lack of significant reduction can be attributed to the inherent uncertainty in the pool and the production of the PV unit, which cannot be effectively mitigated through alternative procurement options in these two specific cases. Additionally, it is important to note that in the *NoGrid* case, where participation in the pool is not considered and there are no associated operational costs for the power production of the self-generation PV facility, the operation costs across each scenario are identical. As a result, the expected cost and the CVaR coincide in this particular case.

Table 6 provides the overall expected costs for each case. These costs comprise the investment costs for the self-generation PV facility and batteries, expenses related to grid-contracted power, expected costs of pool purchases, expenditures tied to energy procured through PPAs, and expected minus revenues from selling energy to the pool. Note that the penalties for unserved demand are not included in this table because they are equal to zero for all analyzed cases. The analysis of these results reveals that the pool and the self-generation PV unit emerge as the primary sources for procurement when available. Notably, as the risk aversion

TABLE 6. Total costs (thousand €).

Case	β	PV	Batt.	Power C.	Pool (p.)	PPA	Pool (s.)	Total
Rel	1	1055.4	0.0	271.3	1729.8	0.0	-10.7	3045.8
	0	1055.4	0.0	227.7	594.1	1572.5	-156.7	3292.9
BAU	1	1055.4	0.0	387.2	2090.4	0.0	-202.9	3330.2
	0	1055.4	0.0	401.0	1104.7	1641.9	-323.7	3879.3
OnlyP	0-1	0.0	0.0	477.1	3984.1	0.0	0.0	4461.2
NoGrid	0-1	4843.7	4260.1	0.0	0.0	0.0	0.0	9103.8

TABLE 7. First-stage decisions.

Case	β	PV (MW)	Batt. (MW / MWh)	PPA (MW)			Power contracted (MW)					
				c_1	c_2	c_3	k_1	k_2	k_3	k_4	k_5	k_6
Rel	1	15.0	0.0 / 0.0	0.0	0.0	0.0	1.5	4.0	6.9	8.8	8.8	8.8
	0	15.0	0.0 / 0.0	2.4	0.0	0.0	2.4	2.4	4.2	8.3	8.3	8.3
BAU	1	15.0	0.0 / 0.0	0.0	0.0	0.0	5.7	5.7	7.4	8.4	8.4	8.4
	0	15.0	0.0 / 0.0	2.5	0.0	0.0	6.1	6.1	7.7	8.1	8.1	8.1
OnlyP	0-1	0.0	0.0 / 0.0	0.0	0.0	0.0	6.7	7.8	9.3	9.7	9.7	9.7
NoGrid	0-1	68.8	12.7 / 110.7	0.0	0.0	0.0	0.0	0.0	0.0	0.0	0.0	0.0

parameter (β) decreases, signifying an increase in the cement producer's risk aversion, the cost associated with energy procurement from the pool decreases. This reduction is a strategic response aimed at mitigating exposure to uncertainty in pool prices. Additionally, it is noteworthy that PPAs serve as effective instruments for mitigating high costs in the most unfavorable scenarios. As a consequence of this, these agreements are only used when the cement producer adopts a risk-averse perspective.

Table 7 provides the first-stage decision variables for each examined case. These variables encompass the installed capacity of the self-generation PV facility and batteries, the power procured through PPAs, and the power capacity contracted with the grid. The values presented in this table align with those detailed in Table 6. Notably, in both the *Rel* and *BAU* cases, the capacity installed from the self-generation PV unit reaches its upper limit. This highlights the self-generation PV unit's efficacy as a compelling electricity procurement tool for the cement producer within the specified location and under the given capital costs. It's important to note that batteries are exclusively deployed when the cement plant operates independently of the grid. This decision may stem from the current high capital costs associated with these storage units, rendering them less financially viable at present. Lastly, it is observed that the contracted power during peak-price periods (k_1 and k_2) is notably smaller than in other periods. This outcome signifies the flexibility of the production process, allowing the cement producer to adapt and capitalize on lower power contracting costs.

Table 8 depicts the total annual energy corresponding to each electricity procurement option. Specifically, it presents the expected energy acquired from the pool and PPAs, the output from the self-generation PV unit, the energy discharged and charged from the battery, and the energy sold to the pool. Observe that the energy obtained from the pool

TABLE 8. Energy (GWh).

Case	β	Pool (p.)	PPA	PV	Batt. (d.)	Batt. (c.)	Pool (s.)
Rel	1	27.9	0.0	27.0	0.0	0.0	0.2
	0	10.7	21.0	26.7	0.0	0.0	3.4
BAU	1	32.0	0.0	27.0	0.0	0.0	4.2
	0	16.8	21.9	23.1	0.0	0.0	6.7
OnlyP	0-1	58.7	0.0	0.0	0.0	0.0	0.0
NoGrid	0-1	0.0	0.0	65.3	22.5	27.7	0.0

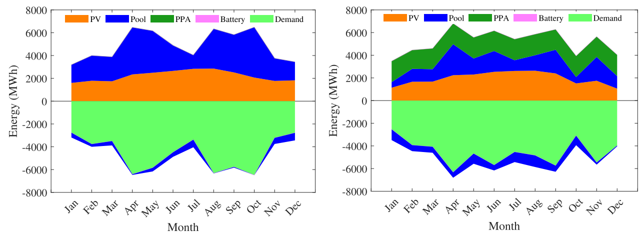

(a) Risk neutral ($\beta = 1$) (b) Risk averse ($\beta = 0$)

FIGURE 13. Energy generation per month (*BAU*).

is reduced when risk is accounted for, $\beta = 0$, with respect to the risk-neutral cases ($\beta = 1$). As mentioned before, the participation in the pool is the major uncertain source in the electricity procurement problem of the cement producer. We observe also that most of the energy is obtained from the self-production unit in all cases in which it is available. Finally, it is interesting to note in *NoGrid* case that almost half of the PV production is stored in the batteries for latter use.

Fig. 13 presents, for the same case, an overview of aggregated monthly energy generation and consumption for $\beta = \{0, 1\}$. Within this depiction, it becomes apparent that monthly PV productions tend to be smaller than the corresponding monthly demands. Notably, the monthly output of the PV unit exhibits a significant increase during summer months compared to winter months. Furthermore, variations in demand throughout the year are evident, with high demand values observed in April and May, among others. During these months, the PV availability is high, and pool prices are relatively low, as corroborated by Figs. 8 and 10b. Upon comparing Figs. 13a and 13b, it is observed that the energy purchased from the pool significantly decreases as risk is taken into account ($\beta = 0$). The reduction in pool purchases is compensated by the acquisition of energy through PPAs, which represent a risk-free source of power.

As an illustrative example, the operation of the kiln is showcased in Fig. 14 for the *BAU* case and $\beta = 1$. This process is selected due to its pivotal role in cement manufacturing. The operational status of the kiln is detailed in Fig. 14a, revealing two maintenance intervals lasting 14 and 25 days, occurring at periods 275 and 623, respectively. The power consumption profile for the kiln is presented in Fig. 14b, highlighting maximum and minimum power consumption of 4000 and 3600 kW, respectively. The

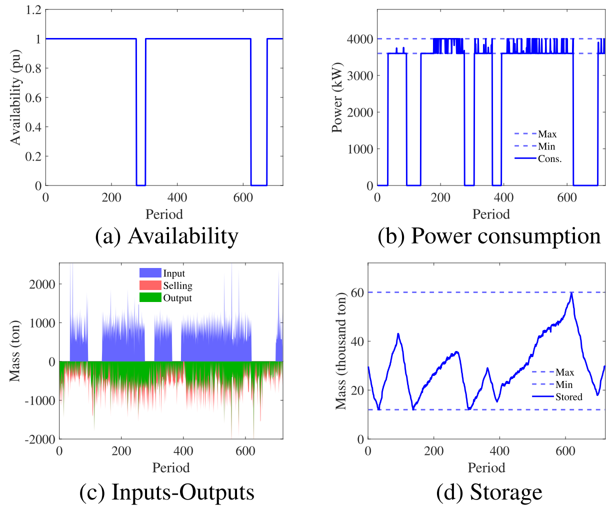

(a) Availability (b) Power consumption (c) Inputs-Outputs (d) Storage

FIGURE 14. Kiln operation in *BAU* case and $\beta = 1$.

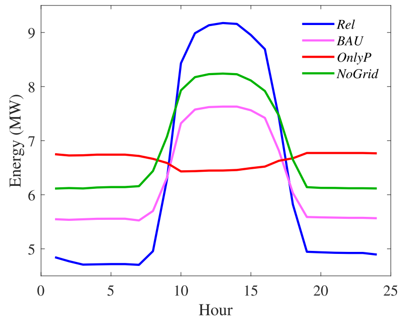

FIGURE 15. Annual hourly consumption for $\beta = 1$ and scenario 1.

kiln operates within its defined power capacity range, and minimum up and down times prevent frequent startups and shutdowns, resulting in only three stops throughout the entire year. Fig. 14c illustrates the mass balance of the kiln storage for each period, showing close ties between input-output patterns and total power consumption. Notably, even during extended shutdowns, the stored clinker quantity is sufficient to meet subsequent process requirements and fulfill client orders. Fig. 14d depicts the clinker quantity stored in each period. Due to the kiln's high minimum power consumption and long up and down times, the storage quantity exhibits stable, incremental, and decremental trends, aligning with startups and shutdowns.

Fig. 15 illustrates the average hourly power consumption throughout the year for all cases at $\beta = 1$ in scenario 1. These charts are derived by converting the 720 non-hourly demand values into 8760 hourly values. The resulting series is organized by computing the average value of the 365 daily vectors, each containing 24 hourly values. The purpose of this figure is to demonstrate the flexibility of the total cement plant power consumption in adapting over time to the most economical energy sources.

Then, Fig. 15 reveals that energy consumption remains relatively stable during the day in the case *OnlyP*, with the peak occurring during nighttime when electricity prices are lower. Conversely, Fig. 15 demonstrates the opposite effect for the rest of the cases, with the highest energy consumption concentrated in the central part of the day when solar PV production is at its peak. It is also observed that the case *Rel* is the case in which the consumption of the cement plant is more able to adapt to the curve of solar PV production. If the curves of *Rel* and *BAU* are compared, it can be stated that the solution of case *Rel* overestimates the flexibility of the cement plant. Observe that the annual hourly consumption in the case *NoGrid* is higher than the energy consumed in the case *BAU*. This is consistent with the fact that energy cannot be sold to the pool in the former case. Finally, it can be concluded that optimizing the power consumption during the cement plant manufacturing process is viable, allowing for adaptation to more cost-effective power sources in each specific scenario.

VII. SENSITIVITY ANALYSIS

This section presents the outcomes of three distinct sensitivity analyses, each focused on examining the expected cost and CVaR in response to variations in different parameters. The initial sensitivity analysis assesses the implications of adjusting the weighting parameter β, which characterizes the tradeoff between expected costs and CVaR. The following two analyses investigate the impact of altering the number of time periods and scenarios on both the expected cost and CVaR, respectively. All simulations were executed using CPLEX 12.6.1 on a HPE ProLiant DL560 Gen11 server, equipped with four 2.2GHz 18-core processors and 512 GB of RAM.

A. WEIGHTING PARAMETER β

The parameter $\beta \in [0, 1]$ in the objective function (28) serves to characterize the level of risk aversion faced by the decision maker. Values of β in proximity to 1 signify a risk-neutral position, emphasizing the minimization of the expected cost for the cement plant. Conversely, values of β nearing 0 reflect risk-averse positions, prioritizing the reduction of expected costs in worst scenarios, characterized by the CVaR. In this subsection, we analyze the impact of the parameter β in the *BAU* case. The pair expected cost and CVaR resulting from an optimal solution for a given value of β is referred to as efficient point, in such a way that is not possible to find a set of optimization variables resulting simultaneously in lower expected cost and CVaR. The ensemble of efficient points is denoted as efficient frontier. Figure 16 illustrates the efficient frontier for the *BAU* case. Notably, the CVaR decreases as the expected cost increases. From the decision maker's perspective, transitioning from the solution at $\beta = 1$ to $\beta = 0.5$ could be of interest, as it allows for a 1.9% reduction in CVaR with only a marginal 0.8% increase in expected cost. However, it is less advantageous to move from $\beta = 0.25$ to $\beta = 0$, as this would incur a 7.5% rise in expected cost while achieving a mere 0.03% reduction in CVaR.

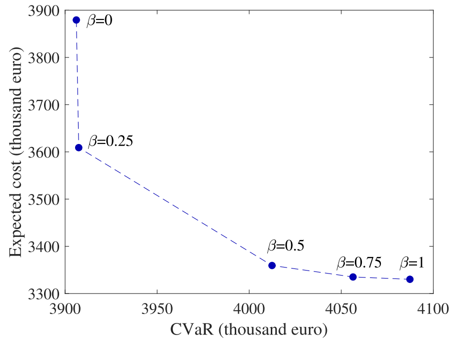

FIGURE 16. **Efficient frontier for case *BAU*.**

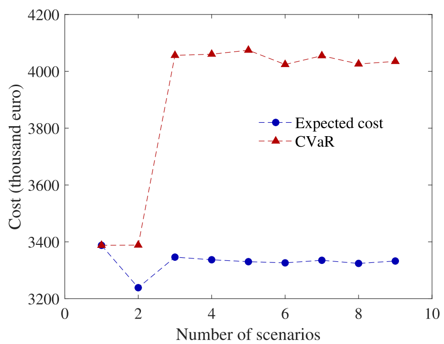

FIGURE 17. **Expected cost and CVaR for different number of scenarios (*BAU*).**

B. NUMBER OF SCENARIOS

In this analysis, we aim to quantify the influence of the number of scenarios on the resulting expected cost and CVaR. As outlined in Sections IV-K and V-I, we employ the scenario reduction technique proposed by [25] to trim the initial set of nine scenarios. Figure 17 depicts the expected cost and the CVaR for different numbers of scenarios in the *BAU* case. This figure illustrates that both expected cost and CVaR exhibit considerable stability for scenarios exceeding 3. Notably, the expected cost, derived from considering all scenarios, demonstrates more robust stability compared to the CVaR across different scenario quantities. For example, the shift from 5 scenarios to 9 results in a marginal 0.07% difference in expected cost, whereas the CVaR experiences a more pronounced 0.97% variation.

C. NUMBER OF TIME PERIODS

This final sensitivity analysis is focused in determining the impact of varying the number of time periods on both the expected cost and CVaR. As explained in Section IV-K, we employ a chronological time-period clustering as outlined in [23] to manage the computational complexity of the resulting optimization problem. To assess the influence of the number of time periods on the expected cost and CVaR, the *BAU* case is solved for various time periods. To ensure comparability across problems with different numbers of time periods, we omit constraints related to minimum up and down times and maintenance periods. These constraints,

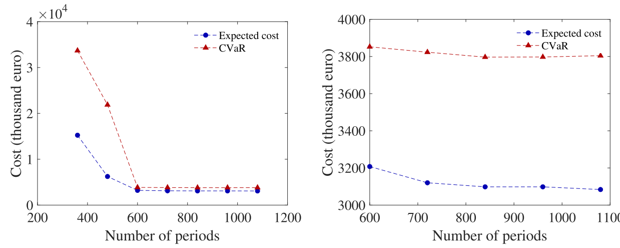

(a) 360-1080 periods
(b) 600-1080 periods

FIGURE 18. **Expected cost and CVaR for different number of timpe periods (*BAU* without minimum up and down times and maintenance periods).**

when retained with a small number of time periods, could lead to infeasibilities and unrealistic up, down and maintenance durations. Figure 18 displays the evolution of expected cost and CVaR for different periods, ranging from 360 (15×24) to 1080 (45×24). In Figure 18a, high costs are observed for numbers of periods below 360, attributed to unserved quantities of the product which are penalized in the objective function (28). This arises from excessively large values of the duration parameter $\Delta_{t\omega}$ when the number of periods is too low, causing certain storages, particularly the one located in the expedition section, to reach maximum capacity in some periods, hindering the production and storage of additional products to be used in following periods. Figure 18b reveals that expected cost and CVaR exhibit stability for numbers of periods exceeding 720. Notably, the difference between expected cost and CVaR for 720 and 1080 numbers of periods is only 1.2% and 0.5%, respectively.

VIII. CONCLUSION

This work introduces a novel procedure for determining the medium-term electricity procurement strategy for cement plants. The proposed approach encompasses participation in the energy pool, photovoltaic self-generation, battery usage, and power-purchase agreements. The mathematical model developed captures operational characteristics and consumption patterns across various stages of cement production, while also accounting for uncertainties in electricity prices and solar photovoltaic production. To make the problem computationally feasible, it is necessary to reduce the initial number of 8760 hourly periods that characterize the planning horizon to a more manageable set of representative periods. The proposed approach utilizes a methodology based on chronological time periods to cluster adjacent hourly intervals into non-hourly periods. It is important to note that using a continuous-relaxed version of the original mixed-integer linear programming formulation results in a substantial underestimation of both the expected value and the CVaR of the cost. The adjustment of the weighting parameter between expected cost and the CVaR allows for a change in the risk-aversion position of the cement plant manager. Although the solution times associated with the proposed approach are relatively high, ranging from several hours to several days, they remain reasonable for addressing a medium-term decision-making problem.

A practical case study was conducted using data from an operational cement plant in Spain, and the key findings derived from this analysis are described below. It is important to note that these conclusions can only be applied to the particular case study that is solved here and cannot be extrapolated to other cases with different electricity prices, solar PV resources, or cement plant characteristics.

- Solely participating in the pool increases significantly the expected value and the CVaR of procurement costs compared to the case where alternative procurement options are available.
- The installation of a solar photovoltaic system proves economically viable for the considered cement producer, leading to a significant reduction in the expected procurement cost compared to cases without this installation.
- At current capital costs, the installation of batteries cannot be considered as economically viable for the considered cement producer.
- The uncertainty of pool prices exerts a more pronounced influence on procurement costs compared to the uncertainty associated with the self-generation PV unit's production.
- High costs in the least favorable scenarios are mitigated through the use of PPAs.
- The flexibility inherent in the processes of cement manufacturing enables a substantial reduction in contracted power during high-price periods.
- The power consumption linked to the cement plant's manufacturing process can be adjusted to leverage more economical power sources in each instance, leading to potential cost savings.
- Sensitivity analyses are essential for appropriately adjusting the number of scenarios and time periods considered in the problem.

Future research lines for this work involve applying the proposed cement plant model to various problems associated with the involvement of cement producers in diverse electricity markets. Ongoing research is focused on developing tools to determine the participation of cement producers in tertiary reserve markets and active demand programs.

REFERENCES

[1] M. Boyer and J.-P. Ponssard. (Dec. 2013). *Economic Analysis of the European Cement Industry*. HAL. Accessed: Dec. 12, 2023. [Online]. Available: https://hal.science/hal-00915646

[2] Y. Liu and X. Guan, "Purchase allocation and demand bidding in electric power markets," *IEEE Trans. Power Syst.*, vol. 18, no. 1, pp. 106–112, Feb. 2003.

[3] E. Gómez-Villalva and A. Ramos, "Optimal energy management of an industrial consumer in liberalized markets," *IEEE Trans. Power Syst.*, vol. 18, no. 2, pp. 716–723, May 2003.

[4] A. J. Conejo, J. J. Fernández-González, and N. Alguacil, "Energy procurement for large consumers in electricity markets," *IEE Proc.-Gener., Transmiss. Distrib.*, vol. 152, no. 3, pp. 357–364, May 2005.

[5] M. Carrión, A. B. Philpott, A. J. Conejo, and J. M. Arroyo, "A stochastic programming approach to electric energy procurement for large consumers," *IEEE Trans. Power Syst.*, vol. 22, no. 2, pp. 744–754, May 2007.

[6] R. Pedrini, E. C. Finardi, and D. S. Ramos, "Hedging power market risk by investing in self-production from complementing renewable sources," *Electr. Power Syst. Res.*, vol. 189, Dec. 2020, Art. no. 106669.

[7] F. Angizeh and M. Parvania, "Stochastic risk-based flexibility scheduling for large customers with onsite solar generation," *IET Renew. Power Gener.*, vol. 13, no. 14, pp. 2705–2714, Oct. 2019.

[8] D. A. Lima and A. M. Céspedes, "Stochastic analysis of economic viability of photovoltaic panels installation for big consumers in Brazil," *Electr. Power Syst. Res.*, vol. 173, pp. 164–172, Aug. 2019.

[9] S. Nojavan and H. Aalami, "Stochastic energy procurement of large electricity consumer considering photovoltaic, wind-turbine, micro-turbines, energy storage system in the presence of demand response program," *Energy Convers. Manag.*, vol. 103, pp. 1008–1018, Oct. 2015.

[10] B. Ceran, "The concept of use of PV/WT/FC hybrid power generation system for smoothing the energy profile of the consumer," *Energy*, vol. 167, pp. 853–865, Jan. 2019.

[11] J. Arellano and M. Carrión, "Electricity procurement of large consumers considering power-purchase agreements, *Energy Rep.*, vol. 9, pp. 5384–5396, Dec. 2023.

[12] M. Shafie-khah, P. Siano, J. Aghaei, M. A. S. Masoum, F. Li, and J. P. S. Catalão, "Comprehensive review of the recent advances in industrial and commercial DR," *IEEE Trans. Ind. Informat.*, vol. 15, no. 7, pp. 3757–3771, Jul. 2019.

[13] Q. Zhang, A. M. Bremen, I. E. Grossmann, and J. M. Pinto, "Long-term electricity procurement for large industrial consumers under uncertainty," *Ind. Eng. Chem. Res.*, vol. 57, no. 9, pp. 3333–3347, Feb. 2018.

[14] X. Zhang, G. Hug, Z. Kolter, and I. Harjunkoski, "Industrial demand response by steel plants with spinning reserve provision," in *Proc. North Amer. Power Symp. (NAPS)*, Charlotte, NC, USA, Oct. 2015, pp. 1–6.

[15] Y. Zhou, P. Su, J. Wu, W. Sun, X. Xu, and M. Abeysekera, "Digital twins for flexibility service provision from industrial energy systems," in *Proc. IEEE 1st Int. Conf. Digit. Twins Parallel Intell. (DTPI)*, Beijing, China, Jul. 2021, pp. 274–277.

[16] C. Manna, M. Lahariya, F. Karami, and C. Develder, "A data-driven optimization framework for industrial demand-side flexibility," *Energy*, vol. 278, Sep. 2023, Art. no. 127737.

[17] J. Wilson and H. C. Iten, "Optimizing energy utilization in cement plant operations," *IEEE Trans. Ind. Appl.*, vol. IA-12, no. 5, pp. 529–535, Sep. 1976.

[18] M. Schneider, V. Hoenig, J. Ruppert, and J. Rickert, "The cement plant of tomorrow," *Cement Concrete Res.*, vol. 173, Nov. 2023, Art. no. 107290.

[19] X. Zhang, G. Hug, J. Z. Kolter, and I. Harjunkoski, "Demand response of ancillary service from industrial loads coordinated with energy storage," *IEEE Trans. Power Syst.*, vol. 33, no. 1, pp. 951–961, Jan. 2018.

[20] E. Allevi, A. J. Conejo, G. Oggioni, R. Riccardi, and C. Ruiz, "Evaluating the strategic behavior of cement producers: An equilibrium problem with equilibrium constraints," *Eur. J. Oper. Res.*, vol. 264, no. 2, pp. 717–731, Jan. 2018.

[21] A. J. Conejo, M. Carrión, and J. M. Morales, *Decision Making Under Uncertainty in Electricity Markets*. Berlin, Germany: Springer, 2010.

[22] R. T. Rockafellar and S. Uryasev, "Conditional value-at-risk for general loss distributions," *J. Banking Finance*, vol. 26, no. 7, pp. 1443–1471, Jul. 2002.

[23] S. Pineda and J. M. Morales, "Chronological time-period clustering for optimal capacity expansion planning with storage," *IEEE Trans. Power Syst.*, vol. 33, no. 6, pp. 7162–7170, Nov. 2018.

[24] M. Hoffmann, L. Kotzur, D. Stolten, and M. Robinius, "A review on time series aggregation methods for energy system models," *Energies*, vol. 13, no. 3, p. 641, Feb. 2020.

[25] J. M. Morales, S. Pineda, A. J. Conejo, and M. Carrión, "Scenario reduction for futures market trading in electricity markets," *IEEE Trans. Power Syst.*, vol. 24, no. 2, pp. 878–888, May 2009.

[26] Spanish National Markets and Competition Commission (CNMC). (Jun. 2021). *La Nueva Factura de la luz–7. INDUSTRIAS (Tarifas 6.1 a 6.4)*. Accessed: Dec. 12, 2023. [Online]. Available: https://www.cnmc.es/file/305276/download

[27] *Spanish Electricity Market Operator (OMIE)*. Accessed: Dec. 12, 2023. [Online]. Available: https://www.omie.es/en

[28] N. Gröwe-Kuska, H. Heitsch, and W. Römisch, "Scenario reduction and scenario tree construction for power management problems," in *Proc. IEEE Bologna Power Tech Conf.*, Bologna, Italy, Jun. 2003, pp. 1–7.
[29] European Commission. *Photovoltaic Geographical Information System (PVGIS)*. Accessed: Dec. 12, 2023. [Online]. Available: https://joint-research-centre.ec.europa.eu/photovoltaic-geographical-information-system-pvgis_en
[30] H. M. Steiner, *Engineering Economic Principles*. New York, NY, USA: McGraw-Hill, 1988.
[31] K. Mongird, V. Viswanathan, P. Balducci, J. Alam, V. Fotedar, V. Koritarov, and B. Hadjerioua, "An evaluation of energy storage cost and performance characteristics," *Energies*, vol. 13, no. 13, p. 3307, Jun. 2020.

JOSÉ ARELLANO received the Ingeniero Técnico Industrial degree from Universidad de Castilla–La Mancha, Toledo, Spain, in 1995, and the Ingeniero Industrial degree from Universidad Politécnica de Valencia, Valencia, Spain, in 2002. He is currently pursuing the Ph.D. degree with Universidad de Castilla–La Mancha. His research interests include power systems economics and stochastic programming.

MIGUEL CARRIÓN (Member, IEEE) received the Ingeniero Industrial and Ph.D. degrees from Universidad de Castilla–La Mancha, Ciudad Real, Spain, in 2003 and 2008, respectively. He is currently an Associate Professor with Universidad de Castilla–La Mancha. His research interests include power systems economics and stochastic programming.

ÁLVARO GARCÍA-CEREZO (Member, IEEE) received the B.Sc. degree in electrical engineering, the M.Sc. degree in industrial engineering, and the Ph.D. degree in science and technologies applied to industrial engineering from Universidad de Castilla–La Mancha, Ciudad Real, Spain, in 2018, 2020, and 2022, respectively. He is currently an Assistant Professor with Universidad de Castilla–La Mancha. His research interests include operations and planning of electric energy systems, optimization methods, operational variability, and decision-making under uncertainty.